

Electron-electron-scattering-induced size effects in a two-dimensional wire

L. W. Molenkamp and M. J. M. de Jong*

Philips Research Laboratories, 5656 AA Eindhoven, The Netherlands

(Received 7 October 1993)

The differential resistance of wires defined in the two-dimensional electron gas in an (Al,Ga)As heterostructure is observed to first increase and then decrease with increasing current. It is demonstrated that this behavior results from the interplay of an enhanced electron-electron-scattering rate (due to current heating of the electron gas), and the partly diffusive nature of boundary scattering in the wire. The data are identified as an experimental observation of the Knudsen maximum and the Poiseuille flow regime in electron transport, and confirm an analogy between electron and gas flow that has been anticipated since the 1950s.

In classical diffusive transport, the effects of electron-electron scattering on the resistivity are difficult to observe. The reason is that normal electron-electron scattering (NEES) does not change the total momentum of the electron distribution, while resistive umklapp processes are rare in bulk simple metals.¹ However, it has been pointed out² that NEES should influence the resistance of small wires with nonspecular boundary scattering, provided that the bulk mean free path l_b exceeds the wire width W . At low electron temperatures, NEES causes electrons whose original trajectory is along the wire axis to be deflected towards the boundaries, where their momentum can be dissipated. This process, the electronic analog of the Knudsen effect in gas-flow dynamics, increases the resistivity.³ At higher electron temperatures, the electron collision rate increases strongly, causing an increase in the time needed for the electrons to reach the boundary of the wire. In this regime, where the mean free path l_{ee} between NEES events drops below W , the resistivity actually decreases with increasing electron temperature, a situation known as the Gurzhi effect.⁴ This is the electronic analog of the Poiseuille gas-flow regime.

Experimentally, only indications of NEES effects have been found.² Most experiments were performed on potassium, which to a good approximation has a spherical Fermi surface. However, the observed changes in the resistance as a function of lattice temperature were limited to about 0.01% of the total resistance, because of the limited l_b and the onset of electron-phonon scattering. Yu *et al.*⁵ reported a negative temperature derivative of the resistivity ($d\rho/dT$) of potassium wires at temperatures around and below 1 K. However, an interpretation in terms of the Gurzhi effect was disputed,² since at these temperatures $l_{ee} > W$. In a later publication by Zhao *et al.*,⁶ it was shown that the negative $d\rho/dT$ can be attributed to metallurgical imperfections. Observations of a positive $d\rho/dT$ in wider wires⁶ were interpreted by Movshovitz and Wiser⁷ as a Knudsen-like behavior due to the combination of relatively infrequent, normal electron-electron and electron-phonon collisions. A similar mech-

anism was proposed to explain an anomalously strong positive $d\rho/dT$ in very thin potassium films.^{8,9} However, until now there has been no observation of electronic Poiseuille flow, nor has there been an observation of a "Knudsen maximum" in the resistance¹ at the crossover between Knudsen and Poiseuille flow regimes.

Here, we present a study of Knudsen and Gurzhi phenomena in two-dimensional wires, fabricated from high-mobility (Al,Ga)As heterostructures. Using this material to study NEES effects offers the advantages of a long l_b , the absence of umklapp processes, and a weak electron-phonon coupling. We demonstrate a clear and unambiguous observation of the Knudsen and Poiseuille flow regimes, as well as the Knudsen resistance maximum, in a single experiment. The resistance changes caused by NEES processes can be larger than 10% of the total resistance. We model our observations using a theoretical scheme that allows the calculation of NEES effects on the resistance for arbitrary l_{ee} , l_b , and W . From the magnitude of the Knudsen effect we obtain information on the boundary-scattering parameters.

The wires used for the experiments are defined electrostatically in the two-dimensional electron gas (2DEG) of (Al,Ga)As heterostructures. We use electron-beam lithography to fabricate TiAu gates that define wires of various dimensions. We report in detail on three different samples. Wire I has a width $W = 3.9 \mu\text{m}$, and a length $L = 20.2 \mu\text{m}$. It is fabricated from a wafer of electron density $n = 2.2 \times 10^{11} \text{ cm}^{-2}$ and $l_b = 12.4 \mu\text{m}$. Wires II and III both have $W = 4.0 \mu\text{m}$; wire II has $L = 63.7 \mu\text{m}$, and wire III $L = 127.3 \mu\text{m}$. For wires II and III, $n = 2.7 \times 10^{11} \text{ cm}^{-2}$ and $l_b = 19.7 \mu\text{m}$. Transport measurements are carried out in a cryostat at zero magnetic field. The differential resistance is measured with standard low-frequency lock-in techniques, using a 100 μV ac voltage.

Selective Joule heating of the electron gas in the wire is achieved by passing a dc current I through the wire. Such current heating is possible by virtue of the weak electron-acoustic-phonon coupling in the (Al,Ga)As-2DEG system, and has proven very useful for the study of ther-

moelectric phenomena in nanostructures.^{10,11} The wires studied here are equipped with opposing pairs of quantum point contacts in their boundaries. Since the thermopower of the point contacts is quantized,¹¹ we can determine the electron temperature T in the wire, as a function of I , from a simple thermovoltage measurement, as described previously in Ref. 12. We find that for $|I| \lesssim 20 \mu\text{A}$, and a lattice temperature $T_l \lesssim 2 \text{ K}$, the electron temperature T in the wire is approximately given by

$$T = T_l + (I/W)^2 \rho C, \quad (1)$$

where ρ is the resistivity of the channel. The constant C depends on the wire, and is of order $C \approx 0.05 \text{ m}^2\text{K}/\text{W}$. We have verified that T_l does not increase notably until $|I| \gtrsim 40 \mu\text{A}$ for wire I, and until $|I| \gtrsim 20 \mu\text{A}$ for wires II and III. The electron temperature T is directly related to the electron-electron scattering time τ_{ee} , according to¹³

$$\frac{1}{\tau_{ee}(T)} = \frac{E_F}{h} \left(\frac{k_B T}{E_F} \right)^2 \left[\ln \left(\frac{E_F}{k_B T} \right) + \ln \left(\frac{2q}{k_F} \right) + 1 \right]. \quad (2)$$

Here q is the 2D Thomas-Fermi screening wave vector ($q = me^2/2\pi\epsilon_r\epsilon_0\hbar^2$).

In Fig. 1 we show our data on the differential resistance (dV/dI) of wire I, obtained for T_l between 24.7 K (top trace) and 1.5 K (bottom trace). First, consider the lowest curve in Fig. 1, taken at $T_l = 1.5 \text{ K}$. One observes, at low current levels ($|I| < 8 \mu\text{A}$), a narrow region with *increasing* differential resistance dV/dI , resulting in a resistance maximum at $|I| \approx 8 \mu\text{A}$. For larger currents ($8 \mu\text{A} < |I| < 40 \mu\text{A}$), we have a remarkable *decrease* in dV/dI with increasing $|I|$. Finally, at still larger currents ($|I| \gtrsim 40 \mu\text{A}$), dV/dI increases approximately parabolically with I . Only in this regime, we find from a nearby thermometer that the lattice temperature of the sample increases considerably, implying that the quadratic behavior of dV/dI is due to Joule heating of the lattice, in combination with the linear increase of the 2DEG resistivity due to electron-phonon scattering for $4 \text{ K} < T_l < 40 \text{ K}$.¹⁴

However, for the nonmonotonic behavior of dV/dI at

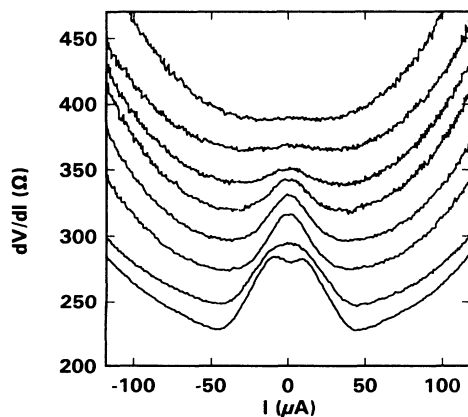


FIG. 1. Differential resistance dV/dI of wire I as a function of heating current I for lattice temperatures of (from top to bottom) 24.7, 20.4, 17.3, 13.6, 10.4, 8.7, 4.4, and 1.5 K.

lower current levels ($I < 40 \mu\text{A}$) lattice heating effects can be ruled out. To see whether NEES could in principle be responsible for our observations in this regime, let us estimate l_{ee} at $|I| \approx 8 \mu\text{A}$. From Eq. (1) we have $T \approx 6 \text{ K}$. Equation (2) then yields $l_{ee} = v_F \tau_{ee} \approx 5 \mu\text{m}$, where v_F is the Fermi velocity. We thus have $l_{ee} \approx W$, roughly the condition one anticipates for the Knudsen resistance maximum. The subsequent decrease in dV/dI we attribute to the Gurzhi effect. For example, for $I = 15 \mu\text{A}$ Eqs. (1) and (2) lead to $l_{ee} \approx 0.8 \mu\text{m} \ll W$, well into the regime of Poiseuille flow. Thus we tentatively assign the increase and decrease of dV/dI at the lowest current levels to the electronic Knudsen and Gurzhi effects, respectively.

As can be observed from Fig. 1, increasing the lattice temperature T_l influences the dV/dI vs I trace in two ways. First, the magnitude of dV/dI at zero heating current increases (note that the data in Fig. 1 are plotted without an additional offset), and second, the NEES features at low current levels disappear with T_l , the Knudsen effect much more rapidly than the Gurzhi effect. This behavior can be understood as resulting from two mechanisms. Due to enhanced electron-phonon scattering l_b decreases with increasing T_l . In addition, a higher T_l also implies a shorter l_{ee} at zero heating current, resulting in a more Poiseuille-like flow pattern in the wire without any current heating.

Obviously, the Knudsen effect can only be observed when $W < l_{ee} < l_b$. These requirements explain why we are only able to observe the positive dV/dI region at the lowest T_l in wire I. In addition, they also imply a much stronger Knudsen effect in samples with larger ratios l_b/W , such as our wires II and III. Data on dV/dI for these samples are shown in Figs. 2(a) (wire II) and 2(b)

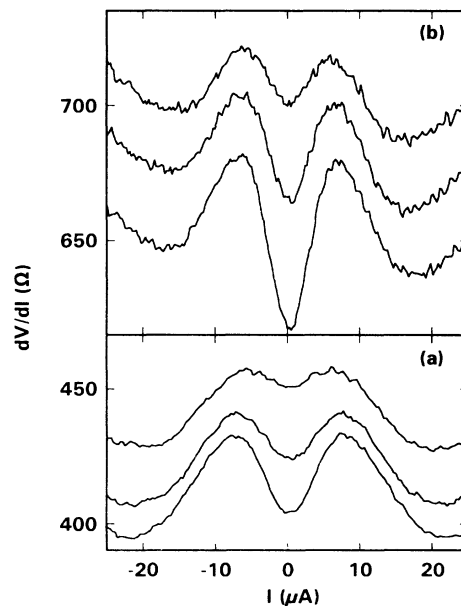


FIG. 2. Differential resistance dV/dI vs I for (a) wire II, and (b) wire III for lattice temperatures of (from top to bottom) 4.5, 3.1, and 1.8 K. At higher current levels, dV/dI exhibits a quasiquadratic increase with current, similar to that in Fig. 1.

(wire III). In these samples the initial increase in dV/dI indeed is much more distinct, leading to a pronounced Knudsen maximum at $|I| \approx 7.5 \mu\text{A}$. Again, the current regimes of increasing and decreasing dV/dI are consistent with the conditions for the electronic Knudsen and Gurzhi effects. Moreover, we see that the total increase in dV/dI in wire III is twice the increase in wire II. This proportionality to L rules out a contact-resistance effect as an explanation for the anomalies. Finally, we remark that in wire III the increase of dV/dI in the Knudsen regime is larger than 10% of the total wire resistance.

To put our interpretation of the experimental data on a more quantitative basis, we have calculated the effects of NEES on the differential resistance of a two-dimensional wire. Calculations starting directly from the Boltzmann equation have only been carried out for certain limiting cases.^{4,15} We have found a solution for arbitrary l_{ee}, l_b , and W using the Chambers method of electron dynamics.¹⁶ Briefly, in this method one follows the path of an electron until it relaxes at an impurity or the bound-

$$l_{\text{eff}}(x) = l - \frac{4l}{\pi} \int_0^1 du \sqrt{1-u^2} \frac{(1-p)e^{-x/lu}}{1-pe^{-W/lu}} + \frac{2}{\pi l_{ee}} \int_0^1 du \frac{\sqrt{1-u^2}}{u} \int_0^W dx' [l_{\text{eff}}(x') + l_{\text{eff}}(W-x')] \left[e^{-(x-x')/lu} \Theta(x-x') + \frac{pe^{-(x+x')/lu}}{1-pe^{-W/lu}} \right], \quad (4)$$

where $l^{-1} = l_b^{-1} + l_{ee}^{-1}$, and $\Theta(x)$ is the unit step function. Finally, the average effective mean free path is obtained from $l_{\text{eff}} = (1/W) \int_0^W dx l_{\text{eff}}(x)$. Note that the first two terms on the right-hand side of Eq. (4) can be interpreted as a two-dimensional version of the Fuchs-Sondheimer equation, while the third term takes the electron-electron scattering into account. We plan to give full details in a future publication. Equation (4) is solved self-consistently using numerical methods. Figure 3 shows a typical result of our calculations for the nonmonotonic dependence of l_{eff} on l_{ee} for given p and l_b , leading to the Knudsen and Gurzhi effects.

To allow a comparison with experiment, l_{ee} is related to I using Eqs. (1)–(3). The resistance of the wire is obtained from $R \equiv V/I = h\pi/2e^2 k_F W + \rho L/W$, where the first term is the two-dimensional Sharvin contact

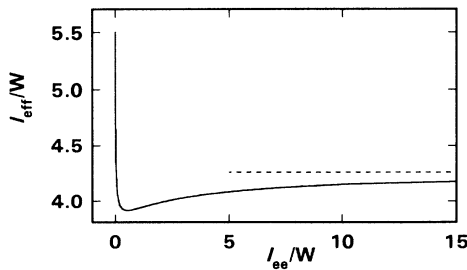


FIG. 3. Calculated dependence of the effective mean free path l_{eff} on the electron-electron-scattering length l_{ee} (both in units of wire width W), for fixed bulk mean free path $l_b = 5.5W$. Boundary scattering is modeled by Eq. (5), with $\alpha = 0.7$. The dashed line indicates the asymptote that l_{eff} approaches for large l_{ee} . Note that for $l_{ee} \rightarrow 0$, $l_{\text{eff}} \rightarrow l_b$.

ary of the system, and then determines a weighted average of the path lengths. The resulting effective mean free path l_{eff} is related to the resistivity ρ of the wire by

$$\rho^{-1} = \frac{ne^2}{mv_F} l_{\text{eff}}. \quad (3)$$

Using this method, Movshovitz and Wiser have obtained analytical expressions for the effective mean free path in a film⁸ and a wire.⁷ However, their calculation includes at most one NEES event per electron trajectory, which limits its application to the range $l_{ee} \gg l_b$, the initial part of the Knudsen regime. We have extended this approach to include multiple NEES events and adapted it to the two-dimensional case. Our formalism allows us to evaluate l_{eff} in the Knudsen and Poiseuille flow regimes without any further approximation. We assume that a fraction p of the incident electrons is reflected specularly at the boundary, the remainder being scattered diffusively, and obtain for the effective mean free path at position x along the width of the wire

resistance.¹⁷ Then, dV/dI is evaluated numerically. In Fig. 4 we compare the lowest-temperature data of Figs. 1 and 2 with the results of our calculation. Note that for all three cases, the calculated dV/dI values are 60–80 Ω smaller than the experimental values. This is due to the resistance of the wide 2DEG leading to the wires, which is

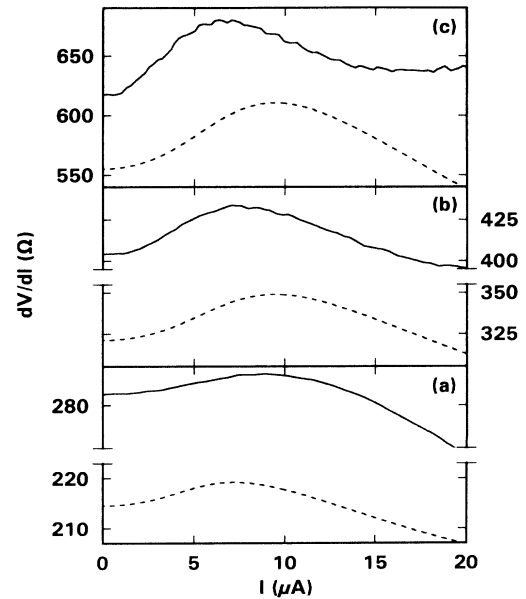


FIG. 4. A comparison of the low-temperature data of (a) wire I (Fig. 1), (b) wire II [Fig. 2(a)], and (c) wire III [Fig. 2(b)] with our calculations. In the calculated curves, the boundary-scattering parameter α is 0.6 for wire I, and 0.7 for wire II. See text for further details.

not included in the calculations. Furthermore, the lattice heating effects at high current levels are not included in our modeling. Apart from this, and given the sample-to-sample variations in the value of parameter C in Eq. (1), the agreement between experiment and theory is striking. To obtain this agreement, we made two further assumptions. First, we assumed that due to depletion the electronic width of the wires is slightly smaller than the lithographic width; we have used $W = l_b/3.5 = 3.5 \mu\text{m}$ for wire I, and $W = l_b/5.5 = 3.6 \mu\text{m}$ for wires II and III. Furthermore, we have found that using a constant value of p for all angles of incidence leads either to a too large value for dV/dI at zero heating current, or a too small Knudsen effect. In reality, p depends on the angle of incidence θ , such that $p \rightarrow 1$ for grazing incidence ($\theta \rightarrow \pm\pi/2$). According to Ref. 18,

$$p(\theta) = \exp[-(\alpha \cos \theta)^2]. \quad (5)$$

Using this expression in Eq. (4) — where $u = \cos \theta$ — we obtain numerical results as in Fig. 4. Good agreement with the experimental data is found with $\alpha = 0.6$ for wire I, and $\alpha = 0.7$ for wires II and III. Theoretically,¹⁸ the parameter $\alpha = 4\pi\delta/\lambda_F$, with δ denoting the root-mean-square boundary roughness. This implies a roughness of about 2.5 nm in our gate-defined wires. Our values for α are much smaller than the typical values ($\alpha \approx 25$) for

potassium wires,⁷ and imply that some 80% of all boundary collisions are specular, consistent with earlier magnetoresistance and electron-focusing experiments.^{19,20} It would be of interest to perform further experiments on wires with boundaries defined by, e.g., reactive ion etching or ion exposure, where boundary scattering is much more diffusive.²⁰

In summary, we have observed a nonmonotonic current dependence of the differential resistance of two-dimensional wires. Quantitative agreement is obtained with a transport theory which combines normal electron-electron scattering with partly diffusive boundary scattering. Taken together, these findings are convincing evidence of the occurrence of electronic Knudsen and Poiseuille transport regimes.

We thank G. E. W. Bauer, C. W. J. Beenakker, and H. van Houten for valuable discussions, and E. E. Bende, O. J. A. Buyk, M. Kemerink, and M. A. A. Mabesoone for technical assistance. The heterostructures were grown by C. T. Foxon at the Philips Research Laboratories in Redhill (Surrey, UK). L.W.M. acknowledges the kind hospitality of Y. Aoyagi, K. Ishibashi, J. Kusano, and S. Namba during a visit to the Laboratory for Quantum Materials, RIKEN, Saitama, Japan, where this research was initiated. M.J.M.d.J. is supported by the Dutch Science Foundation NWO/FOM.

* Also at Instituut-Lorentz, University of Leiden, 2300 RA Leiden, The Netherlands.

¹ J. M. Ziman, *Electrons and Phonons* (Oxford University Press, Oxford, England, 1960).

² M. Kaveh and N. Wiser, *Adv. Phys.* **33**, 257 (1984).

³ J. E. Black, *Phys. Rev. B* **21**, 3279 (1980).

⁴ R. N. Gurzhi, *Zh. Eksp. Teor. Fiz.* **44**, 771 (1963) [*Sov. Phys. JETP* **17**, 521 (1963)]; *Usp. Fiz. Nauk.* **94**, 689 (1968) [*Sov. Phys. Usp.* **11**, 255 (1968)].

⁵ Z. Z. Yu, M. Haerle, J. W. Zwart, J. Bass, W. P. Pratt, Jr., and P. A. Schroeder, *Phys. Rev. Lett.* **52**, 368 (1984).

⁶ J. Zhao, W. P. Pratt, Jr., H. Sato, P. A. Schroeder, and J. Bass, *Phys. Rev. B* **37**, 8738 (1988).

⁷ D. Movshovitz and N. Wiser, *J. Phys. Condens. Matter* **2**, 8053 (1990).

⁸ D. Movshovitz and N. Wiser, *Phys. Rev. B* **41**, 10503 (1990).

⁹ Y.-J. Qian, W. P. Pratt, Jr., P. A. Schroeder, D. Movshovitz, and N. Wiser, *J. Phys. Condens. Matter* **3**, 9459 (1991).

¹⁰ B. L. Gallagher, T. Galloway, P. Beton, J. P. Oxley, S. P. Beaumont, S. Thoms, and C. D. W. Wilkinson, *Phys. Rev. Lett.* **64**, 2058 (1990).

¹¹ L. W. Molenkamp, H. van Houten, C. W. J. Beenakker, R. Eppenga, and C. T. Foxon, *Phys. Rev. Lett.* **65**, 1052

(1990).

¹² L. W. Molenkamp, Th. Gravier, H. van Houten, O. J. A. Buyk, M. A. A. Mabesoone, and C. T. Foxon, *Phys. Rev. Lett.* **68**, 3765 (1992).

¹³ G. F. Giuliani and J. J. Quinn, *Phys. Rev. B* **26**, 4421 (1982). See also A. Yacoby, U. Sivan, C. P. Umbach, and J. M. Hong, *Phys. Rev. Lett.* **66**, 1938 (1991); L. W. Molenkamp, M. J. P. Brugmans, H. van Houten, and C. T. Foxon, *Semicond. Sci. Technol.* **7**, B228 (1992).

¹⁴ T. Kawamura and S. Das Sarma, *Phys. Rev. B* **45**, 3612 (1992).

¹⁵ R. N. Gurzhi, A. N. Kalinenko, and A. I. Kopeliovich, *Zh. Eksp. Teor. Fiz.* **96**, 1522 (1989) [*Sov. Phys. JETP* **69**, 863 (1989)].

¹⁶ R. G. Chambers, *Proc. R. Soc. London Ser. A* **202**, 378 (1950).

¹⁷ M. J. M. de Jong, *Phys. Rev. B* (to be published).

¹⁸ S. B. Soffer, *J. Appl. Phys.* **38**, 1710 (1967).

¹⁹ C. W. J. Beenakker and H. van Houten, in *Solid State Physics: Advances in Research and Applications*, edited by H. Ehrenreich and D. Turnbull (Academic, New York, 1991), Vol. 44, p. 1.

²⁰ T. J. Thornton, M. L. Roukes, A. Scherer, and B. P. Van der Gaag, *Phys. Rev. Lett.* **63**, 2128 (1989).